TOPICAL REVIEW — ZnO-related materials and devices

The p-type ZnO thin films obtained by a reversed substitution doping method of thermal oxidation of Zn_3N_2 precursors*

Bing-Sheng Li(李炳生)[1], Zhi-Yan Xiao(肖芝燕)[2,†], Jian-Gang Ma(马剑刚)[2], and Yi-Chun Liu(刘益春)[2,‡]

[1] Department of physics, School of Sciences, Harbin Institute of Technology, Harbin 150080, China

[2] Key Laboratory of UV Light Emitting Materials and Technology Under Ministry of Education, Northeast Normal University, Changchun 130024, China

(Received 4 May 2017; revised manuscript received 15 June 2017; published online 30 September 2017)

P-type ZnO is crucial for the realization of ZnO-based homojunction ultraviolet optoelectronic devices. The problem associated with the preparation of stable p-type ZnO with high hole density still hinders device applications. In this paper, we introduce an alternative route to stabilizing N in the oxidation process, the thermal stability of p-ZnO is significantly improved. Finally, we discuss the limitations of the alternative doping method and provide some prospective outlook of the method.

Keywords: wide band gap semiconductor, p-ZnO, Zn_3N_2, thermal oxidation

PACS: 71.55.Ht, 72.80.Jc, 73.40.Lq **DOI:** 10.1088/1674-1056/26/11/117101

1. Introduction

With the success of nitride optoelectronics, wide band gap semiconductors have received a great deal of attention due to their various applications. ZnO is a direct wide band gap semiconductor with a large energy gap of 3.37 eV, i.e., in the near-ultraviolet (VU) wavelength region, and a large free exciton binding energy of 60 meV.[1,2] The huge bind energy of the free exciton makes ZnO a promising candidate for the realization of UV emitters based on excitonic emission processes at or above room temperature.[3–9] Furthermore, as with GaN, ZnO also crystallizes into a hexagonal structure. Due to the close lattice matching of each other, the heterojunction between ZnO and GaN has already become an interesting topic in short wavelength semiconductor diodes.[10–15]

ZnO, as a multifunctional semiconductor material, has been known of for more than half a century.[16,17] The recent renaissance of ZnO studies can be retrospected to the mid 1990s and was triggered by the excitonic stimulated emission at high temperature from ZnO single crystal layers, which is contributed by the improvement of the epitaxial technique.[4,5,18] With the introduction of plasma source or laser plume into the film deposition process, the oxygen reactants can be activated and then oxygen vacancies can be sufficiently suppressed, resulting in the formation of stoichiometric ZnO with high structure quality.[19–21] This, in turn, has resulted in an aspiring revival of using ZnO as an optoelectronic material to fabricate short wavelength UV light emitting diodes or lasers.[22–25] Since then, many researchers, motivated by the prospect of using ZnO as a complementary or alternative material to GaN in optoelectronics, have focused on the study of ZnO. So far, ZnO is still one of the research highlights in semiconductor material science, which is witnessed by the numerous conferences, workshops, and symposia and by a huge number of ZnO-related papers published every year. The yearly published papers about ZnO-, GaN-, and ZnSe-related materials in the period of 1980–2015 are shown in Fig. 1. The early research on ZnO can be traced back to the 1930s. The revival occurred in the year 2000, and there have been more than 7000 ZnO-related papers published since 2010.

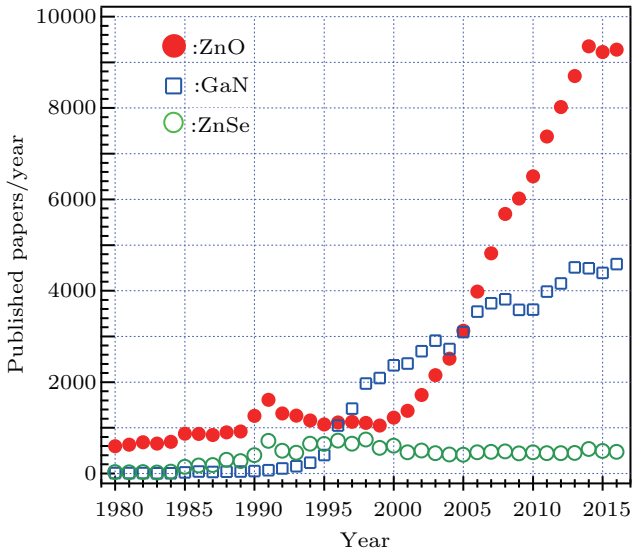


Fig. 1. (color online) Yearly published wide band gap ZnO-, GaN-, and ZnSe-related papers in the period from 1980 to 2015 (from databases of the science web).

Over the past two decades, with tremendous efforts, significant progress has been achieved in ZnO study. The larger

*Project supported by the National Natural Science Foundation of China (Grant No. 11474076).

†Current address: Cincinnati Children's Hospital, UC Health Proton Therapy Center, 777 Yankee Road, Liberty Township, OH, USA 45044

‡Corresponding author. E-mail: ycliu@nenu.edu.cn

© 2017 Chinese Physical Society and IOP Publishing Ltd

bind energy (60 meV) of free exciton is an apparent advantage of ZnO over other wide band gap semiconductors, like GaN (26 meV) and ZnSe (20 meV). Utilizing its high optical gain and exciton effect, several kinds of lasers have been realized with ZnO, such as random lasers,[7,8,26–31] exciton lasers,[2,32–36] exciton-polariton lasers,[37–39] and whispering gallery mode lasers.[40–42] These results have enriched the concepts of semiconductor lasers. It is also worth noting that various novel devices of ZnO-based nanomaterials with distinctive characteristics have been fabricated recently by utilizing the coupled piezoelectric, semiconducting, and excitonic properties.[43,44] Another big advantage of ZnO is the commercial availability of larger single crystal. By employing the hydrothermal method, ZnO single crystal wafers with sizes up to 3 inches in diameter have been available, which provides an ideal platform to realize homoepitaxy of ZnO thin films on native substrates. This can further improve the structural quality of ZnO films with a reduced number of native defects and, consequently, lead to better performances of ZnO-based devices.[45,46] Furthermore, ZnO is amenable to the wet chemical etching, which is particularly important for the device design and fabrication for large scale production.[47] As with GaN-based material system to tune the band gap by alloying with AlN and InN,[48,49] band gap engineering can also be realized in ZnO-based material systems, covering the UV and the whole region of the visible spectrum, by alloying with BeO ($E_g = 10.6$ eV), MgO ($E_g = 7.8$ eV), or CdO ($E_g = 2.4$ eV).[50–54] Enlarging the band gap is usually achieved by increasing the Mg/Zn ratio in $Zn_xMg_{1-x}O$ alloys and the gap is reduced by alloying with CdO. With the improvement of the growth procedure, we have realized ZnO/$Zn_xMg_{1-x}O$ multiple quantum well with high structural quality, in which intersubband absorption in the mid-infrared region has been observed for the first time.[55] This will open up possibilities for applications in the infrared spectral region for ZnO, i.e., optoelectronic devices using intersubband transitions. Because of the large longitudinal optical (LO)-phonon energies of 72 meV, it is possible to develop terahertz QC lasers at high temperature by using ZnO-based quantum structures.[56] Very recently, BeO was also incorporated into the ZnO-based alloys to form a quaternary alloy. Interestingly, it has been found that a "perfect crystal" can be formed by controlling the Be/Mg ratio in $Zn_{1-x-y}Mg_xBe_yO$ quaternary alloy, and overcome the problem of phase separation, caused by high Mg concentration in $Zn_xMg_{1-x}O$ ternary alloy.[57] As indicated by the dotted line in Fig. 2, by adjusting the Be/Mg ratio, the lattice constant of $Zn_{1-x-y}Mg_xBe_yO$ can match that of ZnO. Moreover, the energy band gap can be tuned in a much larger range. This can improve the heterostructure quality and increase the flexibility in device design.

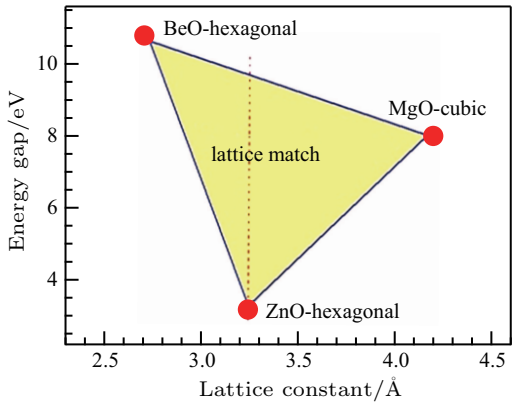


Fig. 2. (color online) Energy band gap versus lattice constants for BeO, ZnO, and MgO. The dotted line indicates that tunability of energy gap of alloys that are lattice-matched to ZnO.

Despite such an attractive potential, the problem associated with the preparation of stable p-type ZnO with high hole density hinders the ZnO-based device application as UV-emitters. So far, substantial studies have focused on this challenging task, and already there have been many reports on the realization of p-type conductivity, and the LEDs of ZnO p/n homojunction.[58–73] However, the reproducibility and stability of p-type ZnO with high hole density still represent unresolved problems.

In this paper, we introduce the method of preparing p-ZnO by oxidizing the Zn_3N_2, which was initially proposed and reported by our group,[74] and report its development. With thermal oxidation treatment, Zn_3N_2 precursor turns into p-type ZnO. The residual N atoms serve as acceptors in ZnO. The major advantage is that the Zn–N bonds have already formed before the doping process and resolved the problem of the low solubility of N-acceptor in ZnO. The P-type ZnO with high carrier density has been obtained by optimizing the oxidation processes. Recently, we carried out the oxidizing procedure on Zn_3N_2:Al and obtained p-type materials.[75] We found that the thermal stability of p-ZnO has been significantly improved by introducing Al into the Zn_3N_2 precursor. Furthermore, the intermediate ternary alloy of ZnON has a tunable band gap in a range of 1.1–3.3 eV. Following the same logic, GaON alloy with a tunable band gap of 2–5 eV has also been realized.[76]

2. ZnO and its p-type doping

For emitters (including LEDs and lasers) with good performance, a ZnO-based p/n homojunction is desired, which is crucial to realizing the efficient carrier injection. This means that both high-quality n-type and p-type materials are required. However, ZnO shows the strong limitation of asymmetric doping. How to overcome this limitation is vital to eventually pushing forward practical device applications. We first briefly present the defects and the p-doping achievements in ZnO. Then we will review the method of oxidizing Zn_3N_2 to realize

p-type ZnO:N: its past, present, and future, its advantage, as well as its limitations.

2.1. Undoped ZnO and its defects

In wide band gap semiconductors, asymmetric doping occurs frequently, i.e., the n-type or p-type is easy to dope, while the opposite type is hardly achievable.[77] The unintentionally doped ZnO shows naturally the n-type conductivity and the n-type conduction with high electron density (up to 10^{21} cm^{-3}) have been achieved by doping group-III (Al, Ga, and In) or group-VII elements, which has been widely used as a transparent conducting oxide electrode in solar cells to replace the expensive indium tin oxide.[78–81] On the other hand, although extensive studies have focused on the p-type doping of ZnO, ZnO-based optoelectronic devices still encounter the p-type ZnO problems. It has been known that the effect of strong self-compensation is the main reason for holding back the realization of p-type ZnO. Usually, the compensation effects in wide band gap semiconductors are related to its native point defects.[82] Therefore, the understanding of the properties of native defects and the mechanism of their formation is the key to realizing p-type conductivity in ZnO. The defects in ZnO have been studied for a long time.[83] However, it is still in debate about their properties.[83–85] In ZnO, the native point defects include zinc interstitials (Zn_i), oxygen interstitials (O_i), oxygen vacancies (V_O), zinc vacancies (V_{Zn}), and Zn_O or O_{Zn} antisites. Among these native point defects, V_O, Zn_i, and Zn_O are the donor-like defects; V_{Zn}, O_i, and O_{Zn} are the acceptor-like defects.[86] The concentration of native defects in a semiconductor is dependent on its formation energy, which can be described with the following formula: $c = N_{\text{sites}} \exp(-E^{\text{f}}/k_{\text{B}}T)$, where N_{sites} and E^{f} are the concentration of sites in the crystal where a defect can occur and the formation energy of the point defects, respectively.[87] Most theoretical calculations have pointed out that the ZnO is of n-type under both Zn-rich and O-rich conditions and cannot be doped into p-type ZnO via native defects (V_{Zn}, O_i, and O_{Zn}).[84] Under zinc rich condition, the native defects of V_O, Zn_i, and Zn_O are abundant due to the low formation enthalpy. Under an oxygen-rich condition, V_{Zn}, and O_i can be formed (O_{Zn} is omitted because of its high formation energy). However, they are compensated for by the defects of V_O, Zn_i, and Zn_O, each of which also has a low formation energy under the O-rich condition. With the introduction of acceptor dopants into crystal, the Fermi energy level will shift toward the valence band edge and results in the further decrease of formation energy for the donor-like native defects. The compensation effect is further enhanced and eliminates the efficient doping ultimately.[88] Therefore, the suppression of native defect formation is essential to the realization of p-type doping in ZnO. It has been reported that single crystal ZnO thin films with electron concentration as low as $n_s \sim 10^{16}$ cm^{-3} and mobility as high as 440 cm^2/V·s have been achieved on a lattice matched substrate, which is necessary for reliable doping.[89]

The origin of n-type conductivity in undoped ZnO is so far still controversial. For a long time, it has been postulated that the unintentional n-type conductivity in ZnO is caused by the presence of native defects of V_O, and Zn_i.[90,91] However, experimental results of optically detected electron paramagnetic resonance measurements on ZnO crystals have demonstrated that these native defects have no contribution to the origin of n-type conductivity in undoped ZnO.[92] Both experimental results[93] and theoretical calculations[87] identified that V_O is the electron-hole radiative recombination center as the source of the green luminescence in ZnO. It has been shown that the V_O is a deep donor and cannot contribute to n-type conductivity.[94] In addition, based on the first-principle calculation results, it has been pointed out that the other donor-like native defects, such as Zn_i and Zn_O, have high formation energies and neither of them is stable in n-type ZnO.[94] Alternatively, another opinion suggested that the origin of n-type conductivity is associated with hydrogen or carbon inside the ZnO.[95,96] Both H_i (interstitial H) and H_O (H substitutes O) act as shallow donors in ZnO. Eliminating the effects of hydrogen, which encroaches in the procedure of ZnO material preparation, device fabrication, and even in the device performance, are big challenges in the future.

2.2. P-doping in ZnO

So far, there have been many reports about ZnO p-type doping prepared by the various thin film growth techniques. Several groups have reported the electroluminescence (EL) of ZnO-based p/n homojunction LEDs.[58–73] However, the device performance is far from final applications. In order to realize p-type doping in ZnO, a variety of acceptors have been employed. For acceptors, one could choose and substitute Zn or O with atoms which have one less electron in the outer shell than the atom which they replace. Following this rule, the group I elements,[60,97–99] including Li, Na, K, Cu, and Ag, and the group V elements, including N, P, As, and Sb, have been selected as acceptors by occupying the Zn site or O site, respectively.[100–102]

Since so many elements among groups I and V can be selected, consequently, a question arises: which one is a good choice as an acceptor dopant in ZnO? From the statistics on the p-type doping in ZnO, it is known that more than half of the reports are about doping with N dopant. Actually, due to the fact that the ionic radius of N is close to that of O, as well as the success of p-type doping in wide band gap II–VI selenides with N dopant,[103] N, provided with N_2, NH_3, N_2O, and NO gas sources, is a natural choice to be an acceptor in ZnO. The p-ZnO:N has been realized by employing a variety of techniques, such as MBE, MOCVD, PLD, laser-MBE,

and sputtering.[45,68,101,104–107] Several groups have fabricated ZnO-based p/n homojunction and realized ultraviolet (UV) EL at room temperature,[22,25,45,108] which further confirmed that the results of p-type ZnO is amenable and ZnO-based emitters have a promising future. Due to the larger exciton binding energy (60 meV), highly efficient emission is expected for the ZnO-based UV emitters. However, at present, to the best of our knowledge, the output power of ZnO light emission diode is extremely low. The main reason is that the low hole concentration leads to a small number of carriers injected into the p/n junction. The x-ray photoelectron spectroscopy and secondary ion mass spectroscopy measurements showed that the N dopant can be doped up to a range of 10^{19}–10^{21} cm^{-3}.[74] One possible reason is that the self- compensation effect results in a huge difference between N dopant concentration and hole concentration in ZnO. Suppressing the formation of native defects in the p-type doping is still a challenge. For intrinsic ZnO, single crystal epitaxial layers with stoichiometry have been obtained. However, the growth window for the 2-dimensional (2-D) layer-by-layer growth mode of ZnO is narrow. For example, *in situ* reflection high-energy electron diffraction (RHEED) used to monitor the growing surface in MBE growth demonstrated that the streaky pattern degraded immediately with the introduction of N gas source, indicating a change of growth mode from two-dimensional (2D) to three-dimensional (3D).[109] As a result, some additional defects have been formed in ZnO. Another possible reason is that the N dopant is not a good acceptor in ZnO. Contrary to what was initially proposed, first-principle calculations based on the hybrid Hartree–Fock density functionals suggested that N is actually a deep acceptor, which is further confirmed by experimental results.[110,111] Many researchers were bewildered by the conflicting experimental results and theoretical expectations. In response to the controversial experimental and calculated results, Liu *et al.* suggested that N_O–V_{Zn} complexes, as a good acceptor, can lead to p-type ZnO.[112] They further figured out how to realize the N_O–V_{Zn} complexes as well as how to avoid the self-compensation effects with controllable processes in epitaxial growth and thermal annealing. Reynolds *et al.* recently demonstrated that p-type ZnO with sufficiently high hole density ($\sim 10^{18}$ cm^{-3}) has been achieved by introducing a shallow acceptor complex V_{Zn}–N_O–H with an ionization energy of 130 meV.[113] However, so far, the lack of follow-up reports and the demonstration of good performance devices based on p–n junctions imply that there may be serious problems with reliability, reproducibility, and stability.

For the other V elements, P, As, and Sb dopants, because their large ionic size mismatches to O, an acceptor with larger ionization energy has been predicted by the theoretical calculation.[114] It has been found that P and As introduced deep acceptor states in ZnSe.[115] Experimentally, however, several groups have realized p-type ZnO via doping P, As, and Sb. The hole density reaches up to $\sim 10^{18}$ or 10^{19} cm^{-3} with low resistivity and high mobility.[100,116–118] The ionization energies of these acceptors are much less than what was expected from theoretical calculations using density functional theory (DFT).[119] Using P, As, and Sb as p-type dopants, the p/n homojunction diodes have been fabricated. These devices exhibited current injection UV light emission in the p/n junction region.[7,100,120] Furthermore, Ryu *et al.* also observed the current injection stimulated emission from ZnO p/n junction.[121] In order to explain the controversial issues between experimental results and DFT theoretical calculations based on the first principle calculations, a new type of acceptor, namely complexes consisting of V elements occupying Zn lattice sites and two nearby Zn vacancies was proposed.[112,114] Recently, Liang *et al.* identified via synchrotron radiation study that the complex defects of acceptors, comprised of substitution Sb ions at Zn sites (Sb_{Zn}) and Zn vacancies within the Sb-doped ZnO lattice, lead to the p-type conductivity.[122] However, Janotti *et al.* pointed out that a large binding energy is required to stabilize these complexes under the equilibrium condition and questioned whether this kind of defect is responsible for p-type conductivity.[123]

Groups Ia (Li, Na, K) and Ib (Cu, Ag, Au) have also been selected for p-type doping in ZnO.[60,72,73,98,99,124–128] The DFT calculation suggested that Li, Na, and K impurities give rise to shallower acceptor levels than the group V impurities, especially P, As, and Sb.[99] There are some reports on the p-type ZnO:Li. However, its hole density is limited to the level of 10^{15}–10^{16} cm^{-3}. The efforts to increase the hole density by introducing more Li atoms into ZnO finally result in semi-insulating ZnO. This is due to the fact that the doped Li atoms play a double role of either a donor or an acceptor in ZnO. The donor behavior arises when Li occurs as an interstitial impurity; the acceptor behavior is exhibited when Li substitutes for a Zn site. Because of the small atomic size, it is favorable for a Li atom to occupy the interstitial position and form a donor. This causes the Fermi level to be between the donor and acceptor levels, i.e., near the midgap. For the Na element doping in ZnO, it is also expected that Na plays an amphoteric role, i.e., an acceptor when substituting for Zn and a donor when occupying interstitial sites. For the K element doping, due to its larger atomic size, it is expected that the amount of interstitial K is suppressed and a p-type ZnO:K has been achieved with the introduction of the K dopant.[129,130] It has been pointed out that the group Ib elements also play roles as acceptors in ZnO.[98,124] A p-type ZnO has been realized with Ag doping.[98] The Cu and Au may act as deep acceptors in ZnO. It has been demonstrated that Cu in ZnO is connected to the green luminescence.[131] In order to increase the hole density, some groups used the double-acceptor co-doping method, that is, Li–N or Ag–N double-acceptor doping, to realize the

p-type ZnO.[73,125] However, there is no sufficient increase in hole density with this method.

3. Thermal oxidation of Zn_3N_2 to fabricate p-type ZnO:N

With tremendous efforts, as mentioned above, great development has been achieved in the preparation of p-type ZnO. However, it is still a big challenge to obtain p-type ZnO with high hole concentration via conventional carrier doping procedure. This is because acceptors with high formation energy, such as N, replace the host O anion in ZnO, which results in the low solubility of dopants. Additionally, the N dopants, are not stable due to the weak chemical bond of Zn–N (dissociation energy $\Delta H_{f298} = 160$ kJ/mol) as compared with that of Zn–O ($H_{f298} = 284$ kJ/mol).[132,133] This is the main reason for p-ZnO to be converted back into n-type with time. How to increase the N solubility and stability is pivotal to achieving the p-type ZnO:N with high hole density. In order to overcome the crucial problem concerning the low solubility of N acceptors in ZnO, we figured out an alternative way to fabricate the p-type ZnO:N by thermally oxidizing Zn_3N_2. We named it a reversed substitution doping (RSD) method to emphasize the difference from the conventional doping, namely the chemical doping (CD) method.

3.1. Zn_3N_2 transforming into p-ZnO:N with O replacing N

Figure 3 is the schematic drawing of basic transformation to realize p-ZnO:N from Zn_3N_2 precursor (left side) and from the conventional doping method (right side). The difference is apparent between the two processes, i.e., the RSD and the CD processes. Usually in the CD process, the N dopant and the O are loaded simultaneously into the chamber during the ZnO thin film deposition. Just as indicated in Fig. 3 (right side), the N dopant will compete with O and occupy the O crystallographic site. Because the electronegativity of oxygen (3.50) is larger than that of nitrogen (3.04), the chemical activity of O is higher than that of N, and Zn preferentially combines with O rather than N. As a result, it is difficult for N to be incorporated into ZnO film, even though N is activated by plasma in the conventional doping procedure. On the other hand, the thermal oxidation of the Zn_3N_2 method can solve this problem, where the low solubility of the N acceptor in ZnO can be solved. As indicated in Fig. 3, the difference between the RSD and CD methods is apparent. Not like in the CD method, where the N replaces O, in the RSD process it is O atoms that replace N atoms. Since the chemical activity of O atoms is higher than that of N atoms, the replacement of N with O is easier to realize with optimizing the oxidation procedure. The residual N atoms in the film will serve as acceptors in ZnO.

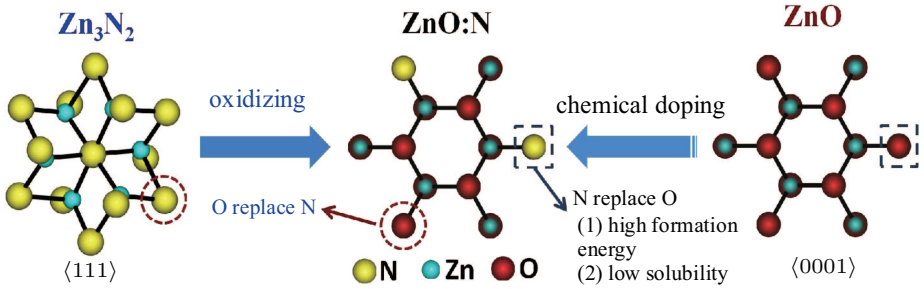


Fig. 3. (color online) Schematic diagram of the p-type ZnO:N fabricated by oxidizing the Zn_3N_2 precursor and the conventional chemical doping methods. Left side: Zn_3N_2 change into p-ZnO:N with oxidizing procedure, in which the N atoms are replaced by O atoms. Right side: the conventional way to fabricate p-ZnO:N with N occupying O lattice sites.

3.2. Development of RSD method

In this subsection, we first introduce a series of our initial results,[74,134–136] followed by the summary of the main achievements by other groups, who also performed the oxidation of Zn_3N_2 to form p-ZnO:N. Next, we present our recent results about p-ZnO prepared by thermal oxidation of Zn_3N_2:Al. We found that the thermal stability of p-type ZnO has been improved by introducing an Al element into Zn_3N_2.[75]

3.2.1. p-type ZnO:N with high hole density fabrication by RSD method

Based on the proposed RSD method, experiments for the synthesis of p-ZnO:N with the oxidation of Zn_3N_2 thin films were first carried out at the beginning of 2002. After that, we carefully confirmed the conduction type and then reported the initial experiments for p-type ZnO:N in 2003.[74] The Zn_3N_2 thin films are deposited on the fused silica substrates at a low temperature of 140 °C with the plasma enhanced chemical vapor deposition (PECVD) system, in which, Diethylzinc (DEZ), NH_3, and high-purity H_2 were loaded as the zinc source, N source, and carrier gas, respectively, for depositing the Zn_3N_2 thin films. After the deposition, thermal oxidation was carried out in an oxygen ambient at different annealing temperatures from 300 to 800 °C for 1 h. The x-ray diffraction (XRD) results demonstrated that the conversion from Zn_3N_2 with a cubic antibixbyite structure to ZnO with hexagonal wurtzite structure occurred at an annealing temperature of 300 °C in the oxygen ambient. The Zn_3N_2

transformed into ZnO entirely when the as-grown film was annealed at 500 °C in an O_2 atmosphere for 1 h. The obtained ZnO thin film possessed a polycrystalline hexagonal wurtzite structure without preferred orientation. With increasing annealing temperature, the intensities of the main peaks increased, and the full width at half-maximum narrowed, which indicates the improvement of structural and crystal quality. Note that the structural properties of ZnO are not only closely dependent on the annealing processes but also related to the Zn_3N_2 itself, which has been confirmed with the following reports on ZnO:N obtained by the RSD method. As shown in Fig. 4. a preferred (002)-oriented ZnO with a narrow linewidth has been obtained.[137] There are actually some tricks in controlling the structural properties. In the as-grown samples, a small amount of O was introduced into the Zn_3N_2 to form ZnON alloy. Then by optimizing the annealing process, the structural quality and orientation can be controlled. We also observed the similar results in the samples prepared by radio frequency reactive magnetron sputtering and plasma-assisted metal-organic chemical vapor deposition.[134,135]

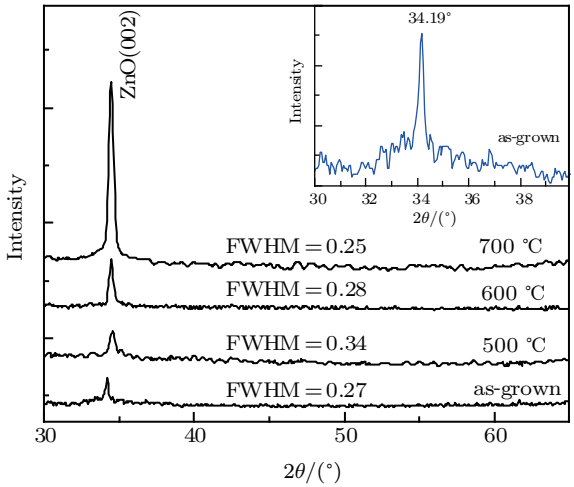


Fig. 4. (color online) XRD curves for the as-grown and annealed samples at different temperatures in oxygen ambient. The annealing temperatures and the linewidths are given and indicated next to their corresponding scan curve. The inset (color online) shows the magnified view of the area around the diffraction peak from the as-grown sample. The peak (located at 34.19°) appears between the ZnO(002) (34.42°) and Zn_3N_2(222) (31.70°) peaks, indicating the formation of Zn–N–O ternary alloy.[137]

After demonstrating that ZnO thin films can be synthetized from thermal oxidation of Zn_3N_2 precursor, we studied the electrical properties of the annealed samples, including resistivity, Hall coefficient, carrier density and mobility, by a Van der Pauw four-point probe Hall system. The four contacts with Au–Cr metals as electrodes were Ohmic, which were confirmed with the linear dependence of *I*–*V* characteristics. The as-grown and annealed samples at 300 and 400 °C are of n-type with the decrease of carrier density from 10^{15} to 10^{12} cm^{-3}. On the contrary, for the samples annealed at 600 and 700 °C, respectively, the Hall coefficient was inverted from negative to positive, indicating a hole-dominant transport. The carrier densities of holes are 1.2×10^{14} and 4.16×10^{17} cm^{-3}, respectively. However, with further increasing the annealing temperature up to 800 °C, the Hall coefficient reversed back to negative, which means that ZnO became n-type again. The dependence of carrier types and densities on the annealing temperatures can be understood from the following explanations. With the increase of annealing temperature in an oxygen ambience, the oxygen atoms intrude into the Zn_3N_2 and replace N atoms to form ZnO. Then the residual N atoms become the dopants in ZnO. Furthermore, the thermal annealing processes can also activate the N-acceptors in ZnO, accompanied by reducing the density of donor-like defects due to the improvement of structural quality. Hence, the density of electrons will decrease with increasing annealing temperature. Finally, the density of acceptors will be dominant, and the ZnO is inverted from n-type to p-type. With a further increase of the annealing temperature (800 °C), the residual N atoms will be further replaced by the oxygen atoms, leading to reconversion of p-type ZnO back to n-type. We also fabricated a ZnO:N/n-Si junction by thermally oxidizing the Zn_3N_2/n-Si heterostructure.[135] In a range of 500–700 °C, all of the junctions show rectifying *I*–*V* characteristics, suggesting that a p-ZnO:N/n-Si hetero-junction has been formed. So far, the problem of p-ZnO stability of electronic properties with N as a dopant also holds back the device application. With the conventional CD method, even if the p-type ZnO is obtained, over time, the conduction type will convert into n-type.[138] The acceptors of N dopants can escape from ZnO due to the weak chemical bond between the N and Zn. We also evaluated the stability of our p-ZnO:N obtained from oxidation of Zn_3N_2 precursor. As shown in Fig. 5, the conduction type and mobility of carriers do not change with time.[136]

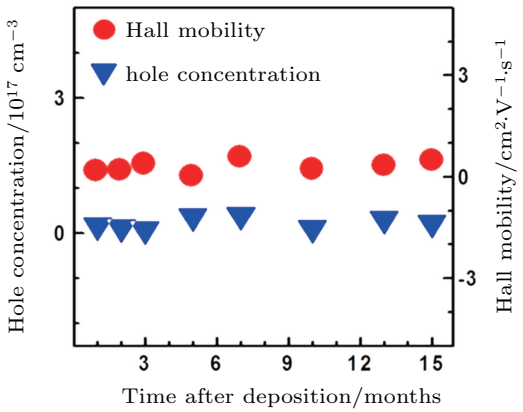


Fig. 5. (color online) Dependence of electronic properties of p-ZnO, obtained from oxidation of Zn_3N_2 precursor, on the time at room temperature. The hole concentration and the mobility keep almost constant with time.[136]

After confirming the p-type ZnO:N with Van der Pauw method, we used x-ray photoelectron spectroscopy (XPS) to evaluate the N concentrations in ZnO obtained from the oxidation of Zn_3N_2 precursor. Shown in Fig. 6 is a typical XPS spectrum of N 1s, centered at 398.33 eV, which corresponds to the N–Zn bond.[74] The outline of the spectrum is asymmetric and there is a shoulder ($\sim$ 400 eV) on the high energy side. This shoulder corresponds to the N–H bond. For the Zn_3N_2 deposition, we use ammonia and hydrogen as the N source and the carrier gas, respectively. A large amount of hydrogen was incorporated into the Zn_3N_2. With the increase of annealing temperature, most of the hydrogen atoms were removed, which had been previously reported by our group.[137] The N concentration is much higher. N concentrations are calculated by using the formula, $C_N = (S_N/\text{asf}_N)/(S_N/\text{asf}_N + S_O/\text{asf}_O + S_{Zn}/\text{asf}_{Zn}) \times 10^{23}$, where S is the integral intensity of the peak for N, Zn, and O elements, and asf is the atomic scattering factor. The N concentrations in the films annealed at 600, 700, and 800 °C are 6.87×10^{21}, 6.78×10^{21}, and 5.48×10^{21} cm^{-3}, respectively. With the increase of annealing temperature, the N concentration decreases, accompanied by the increase of O concentration. These results were further confirmed by the XPS analysis on the ZnO:N samples obtained by thermally oxidizing the Zn_3N_2 thin films deposited by radio frequency reactive magnetron sputtering.[134] We used the Gaussian curve fitting to fit the peak associated with O1s and N1s bonds of the XPS spectra for the samples annealed at various temperatures. The results are summarized in Fig. 7. The results show that the integral intensity of O1s peaks due to Zn–O bonds increases with the increase of annealing temperature. The integral intensity of N1s peaks due to Zn–N bonds, however, decreases monotonically with the increase of the annealing temperature up to 800 °C. When the sample is annealed above 800 °C, N1s intensity is beyond the instrumental limits. These results indicate that the N concentration in ZnO can be controlled by the annealing process. The N dopant concentration increases up to 10^{21} cm^{-3}. This doping level, to the best of our knowledge, is much higher (two orders) than those with conventional doping methods. This demonstrated that the RSD method made a breakthrough in realizing the high N concentration doping in ZnO.

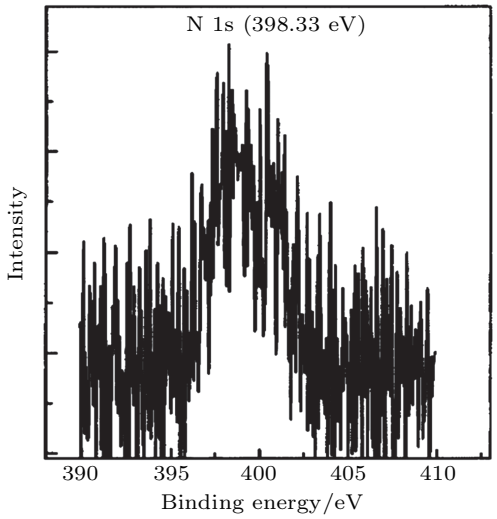


Fig. 6. A typical N 1s spectrum of XPS analysis for ZnO:N prepared by thermal oxidizing Zn_3N_2 precursor at 600 °C in an oxygen ambience for 1 hour.[74]

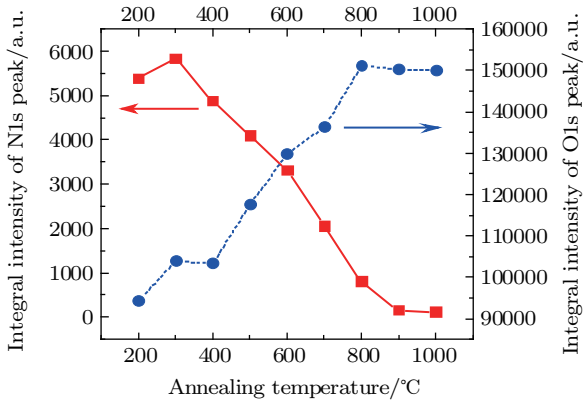


Fig. 7. (color online) Variations of the integral intensities of N 1s and O 1s peaks in XPS spectra with annealing temperature.[134]

The photoluminescence (PL) spectra also suggested the formation of N dopants as acceptors in ZnO prepared by oxidizing the Zn_3N_2 precursor. Figure 8 shows the PL spectra for ZnO:N and intrinsic ZnO thin films prepared by oxidizing the Zn_3N_2 precursor and PECVD, respectively. Shown on the left side are the room temperature PL spectra of p-ZnO:N and undoped ZnO samples. Strong UV band emissions with weak deep level emissions are observed in both samples. However, the differences between their UV bands are apparent. For the undoped one, the linewidth is narrower with a value of 90 meV, while it is 120 meV for p-ZnO. Additionally, a shoulder on the low energy side is shown around 3.2 eV in the p-ZnO sample. The UV band in undoped ZnO originates from the recombination of free excitons. This conclusion is supported by the temperature dependent PL spectra. The inset shows the temperature dependence of the integrated PL intensity in a range of 80 to 580 K. Theoretical simulation (see the caption of Fig. 8) identifies that the activation energy, ΔE, of the thermal quenching process is 61.9 meV, which is in agreement with the exciton binding energy of 60 meV in bulk ZnO crystal. Thus, the UV band of undoped ZnO is from free exciton recombination. For the p-ZnO:N, the temperature dependent PL spectra demonstrate that the UV band is from the overlap between the free exciton and bound exciton. Shown on the right side of Fig. 8 are the low temperature (80 K) PL spectra of ZnO samples prepared at different annealing temperatures. For the p-ZnO annealed at 700 °C, the UV band was resolved as five separate peaks at 3.368, 3.312, 3.239, 3.170,

and 3.100 eV. By judging the peak positions, the emission line at 3.368 eV (P_1) is from free exciton emission because it is in excellent agreement with 3.369 eV from A-exciton recombination in the ZnO bulk crystal.[139] The P_2 emission line at 3.312 eV is the emission line of the exciton bound to the acceptor in ZnO, accompanied by 1 LO, 2 LO, and 3 LO replicas at 3.239, 3.170, and 3.100 eV due to their energy differences, which are consistent with LO-phonon energy of 72 ± 4 meV. Comparing with the undoped sample, a P_2 line appears in N-doped p-ZnO. With the increase of annealing temperature, the P_2 peak nearly disappears. Thus, the P_2 line at the 3.312 line is the exciton emission bound to the neutral N_O-acceptor.

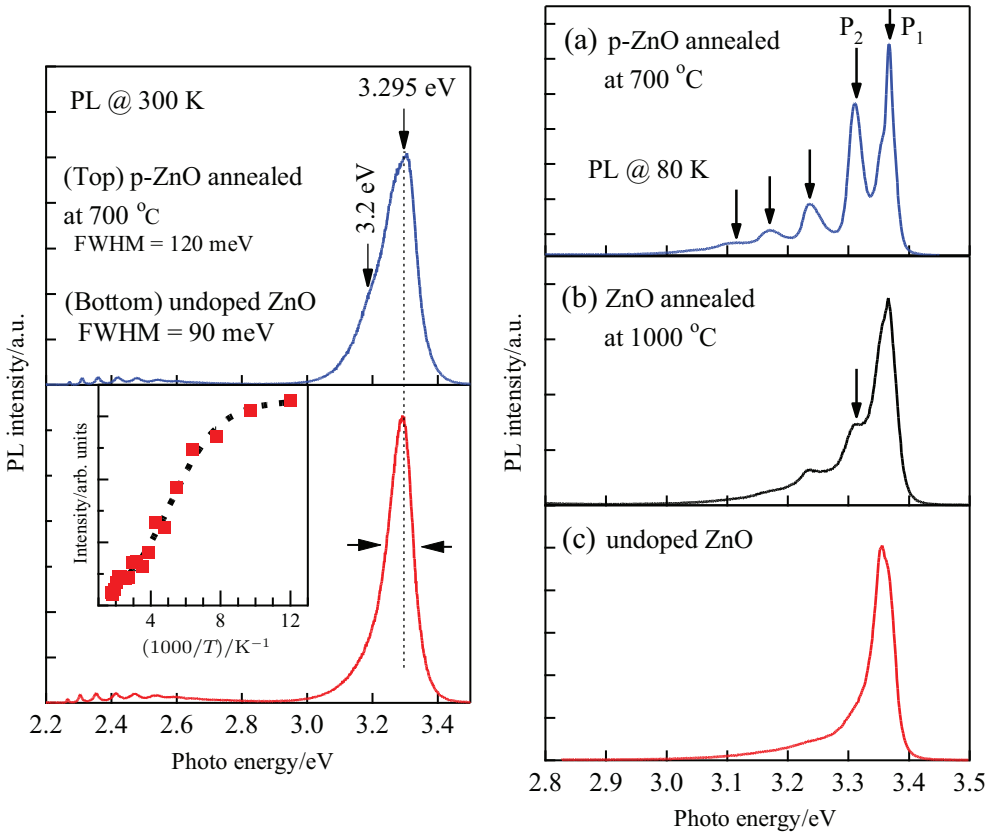


Fig. 8. (color online) Photoluminescence spectra (PL) of ZnO. Left side shows the room temperature PL spectra of the p-type ZnO annealed at 700 °C and undoped ZnO. The inset displays integrated PL intensity dependent on the temperature for the intrinsic ZnO. The squares denote experimental data points. The dotted line represents theoretical fitting by using the equation $I_{(T)} = I_0/[1 + A\exp(-\Delta E/k_B T)]$. Right side shows the low temperature (80 K) PL spectra of ZnO annealed at (a) 700 °C, and (b) 1000 °C, and (c) undoped ZnO.

Table 1. Selected results reported on p-type ZnO prepared by the RSD methods.

Author	Technique	Source	Substrate	R/Ω·cm	Density/cm^{-3}	Year	Ref.
Liu Z W	Sputtering	Zn, N_2	quartz	81	8.12×10^{16}	2007	127
Allenic A	PLD	Zn_3N_2, O_2	Al_2O_3	28	4.9×10^{17}	2007	128
Nakano Y	sputtering	Zn, N_2	quartz	?	$\sim 1\times10^{17}$	2006	129
Jiang N K	sputtering	Zn, N_2	Si, Glass	$\sim 10^{-2}$	$\sim 10^{18} \sim 10^{19}$	2012	130
Zou C W	sputtering	Zn, N_2	Glass	52	8.39×10^{16}	2009	131
Rakhshani A E	sputtering	Zn, N_2	Borosilicate glass	?	5.5×10^{15}	2014	132
Erdogan	PFCVAD	Zn, N_2	Glass	44.5	2.8×10^{17}	2013	133
Jiang N K	sputtering	Zn, N_2	Glass	1.59	7.64×10^{18}	2013	134
Kaminska E	sputtering	Zn, N_2	Al_2O_3, quartz	1.18	6.6×10^{17}	2005	135
Wang C	Sputtering	Zn, N_2	quartz	220	5.78×10^{17}	2003	136
Jin Y P	Sputtering	Zn, N_2	quartz	6.33	8.82×10^{17}	2016	137
Li B S	PECVD	DEZ, NH_3	fused silica	150.05	4.16×10^{17}	2003	63
Xiao Z Y	PECVD	DEZ, NH_3	Si, quartz	1600	2.7×10^{16}	2008	123

The main advantage of the RSD method is the apparent raising of N acceptor solubility in ZnO , which overcomes the bottleneck of the low solubility of N acceptors in ZnO. Thus, this method has been used widely for preparing the p-type ZnO. Based on this method, p-type ZnO:N films with high carrier density have already been achieved. Some results of p-type ZnO prepared by RSD are selected and summarized in Table 1.[74,136,140–150] As seen from Column 5, high-level carrier densities of holes are achieved. Note that the variations of electrical properties are in a wide range, such as resistivity ($10^{-2} \sim 1600\ \Omega$·cm) and hole density ($10^{15} \sim 10^{19}$ cm^{-3}). This is attributed to the complicated process of transformation from Zn_3N_2 to ZnO; it involves several aspects, such as the phase transition, the break of Zn–N bond, the formation of Zn–O bonds, and the activation of the residual N atoms as acceptors, in the transformation process from Zn_3N_2 precursors to ZnO:N films. Each aspect can be affected by the annealing temperature, thermal oxidation time, the annealing method, characteristic of the Zn_3N_2 precursor, as well as the types of substrates.

3.2.2. Improvement of thermal stability of p-ZnO with the introduction Al into Zn_3N_2 precursor

The exploitation of ZnO-based devices requires a lot of processing steps that involve postgrowth annealing cycles at various stages. For example, to make a waveguide structure, the top cladding layer, ZnMgO or ZnMgBeO clad layer, was grown on the top of the ZnO p/n junction, which needs a high temperature. On the other hand, lots of thermal energy will be generated during the device performance, thereby resulting in the increase of device temperature. Therefore, the improvement of thermal stability of p-ZnO is crucial for the ZnO device application. In the thermal oxidation process, the annealing temperature plays an important role in the exchange between N and O atoms in the transformation from Zn_3N_2 to p-type ZnO. The optimized temperature is in a range of 450–600 °C, at which ZnO shows the highest hole density. However, at higher temperature, p-type ZnO reverses back to n-type. The main reason is that the weak chemical bond between the N and Zn:N can be easily replaced by an O element. Thus, it is necessary to improve the thermal stability and to increase the N solubility for achieving stable p-type ZnO. Theoretical calculation suggested that "co-doping" or "cluster doping" of (Ga, N) or (Be, N) can be a better approach to doping the ZnO into p-type ZnO.[151–153] The calculations suggest that cluster doping can reduce the ionized energy of an acceptor and sufficiently increase the dopant solubility due to the low formation enthalpy. The stability of bonded N in ZnO can also be enhanced due to the modified local bonding environment around the dopant.

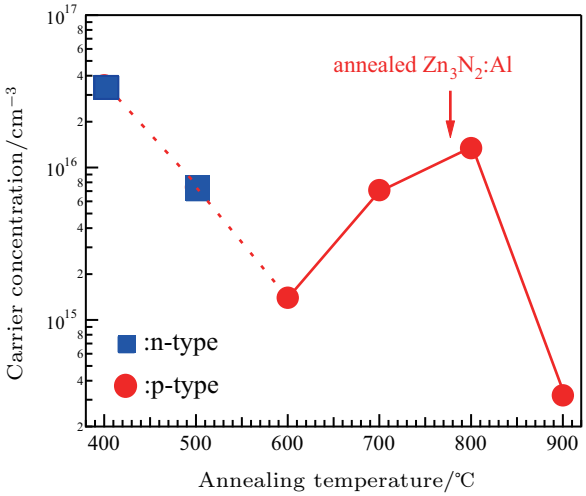


Fig. 9. (color online) Variations of the carrier concentration with annealing temperature for different conduction types of ZnO thin films. The ZnO samples are prepared by oxidizing the Zn_3N_2:Al thin films. The squares represent n-type ZnO and the circles denote p-type ZnO.

In fact, the "co-doping" method of III–V Ga and N was once recognized as an effective method to prepare p-type ZnO.[154] However, the difficulty in controlling the distributions of Ga and N as well as the negative effect of isolated Ga atoms in ZnO resulted in the low reproducibility and preclude its finial practical application. Most calculations and experiments focus on the Ga–N co-doping. We choose and use Al, instead of Ga, due to the fact that the corresponding bonds with N and O are stronger for Al than those for Ga. Thus, the stability and doping concentration of N in ZnO will be further strengthened and increased. The bond dissociation energy, ΔH_{f298}, of Al–N is 297 kJ·mol^{-1}, which is much larger than that of the Zn–N ($\Delta H_{f298} = 160$ kJ·mol^{-1}), even larger than Zn–O ($\Delta H_{f298} = 284$ kJ·mol^{-1}).[133] This indicates that Al can stabilize the doped N in ZnO, if the Al–N is formed. However, the Al itself is a donor-type defect in ZnO. If only a Zn atom is replaced by an Al atom, opposite effect occurs. The Al donors will provide electrons and compensate for the p-type doping. Thus, when using Al to stabilize N in p-type ZnO, the key issues are (i) to reduce the compensation of Al due to the formation of only Al–O bonds; and (ii) to make sure that Al captures more than one N atoms to form AlN2, AlN3, and/or AlN4 in ZnO. In order to avoid having Al atoms acting as donors and to make sure that each Al atom is bonded with more than one N atom, we first prepared Al doped Zn_3N_2 films and then oxidized the films to form ZnO. Ideally, in Al-doped Zn_3N_2, when an Al atom replaces a Zn atom, each Al is completely bonded with 4 N atoms. Since the Al–N bonds are sufficiently strong, they can survive in the transformation of the structure from Zn_3N_2:Al to ZnO during the annealing procedure. The residual N atoms stabilized by Al atom in the newly formed ZnO film may act as acceptors. Figure 9 shows the results of Hall effect measurements for ZnO thin films ob-

tained from oxidizing the Zn_3N_2:Al thin films. For samples obtained from oxidizing Zn_3N_2:Al thin films, they have n-type conductivity at lower annealing temperatures (below 600 °C). The electron concentration decreases with the increase of annealing temperature. The conduction type changes to p-type in the films annealed at 600 °C. The hole density increases in the sample annealed at higher temperature and reaches a maximal value of 1.5×10^{16} cm^{-3} in the sample annealed at 800 °C. The carrier density decreases when the annealing temperature is over 800 °C, but still keeps p-type conductivity till an annealing temperature of 900 °C. In the previous section we discussed that p-type ZnO can be obtained by thermally oxidizing the Zn_3N_2. However, p-type conduction is only obtained in the samples annealed at low temperature. The films convert back to n-type at higher annealing temperature. For Zn_3N_2 material, due to small bond dissociation energy, the chemical bond of Zn–N is easy to break and N atoms are replaced by O atoms even at low annealing temperature. For Zn_3N_2:Al material, a possible explanation is that the Al atoms will stabilize the N atoms, because of the strong Al–N chemical bonds, during the transformation from nitride precursor, to form ZnO:(Al, N_x, $x = 2$, 3, or 4). This is also the reason that the thermal stability is enhanced, compared with previously discussed p-type ZnO obtained from Zn_3N_2 oxidation processes. Although the hole density is still low and further improvement is needed for practical device applications, these results have demonstrated that the properties of ZnO are closely related to the introduction of Al atoms into Zn_3N_2:Al. In order to improve the properties of p-type ZnO, we are now optimizing the concentration of Al dopant in Zn_3N_2:Al, the procedure of thin film deposition and annealing processes to further increase the hole density. Finally, the properties of dopant N in ZnO should be given more discussion. Based on calculated results, the dopant, N, plays a complex role in ZnO, which is closely dependent on the doping procedure. A deep acceptor, N_O, may be formed in Zn-/O-rich condition.[109–111] However, gradually it has been recognized that a shallow acceptor of N_O-complexes can be realized in a special condition.[112,113] In the RSD method, an N-rich ambience can be created and resulting acceptor with small ionization energy will be formed in ZnO. A cluster doping also provides an alternative route to realizing p-ZnO.[151–153]

3.2.3. Limitations of thermal oxidation of Zn_3N_2 precursor to p-ZnO:N

The main breakthrough of the RSD method is to resolve the low solubility of the N acceptors in ZnO. However, several disadvantages of this method are also apparent. First of all, this method of thermal oxidization; phase transformation occurs in the oxidizing process. The Zn_3N_2 has a cubic antibixbyite structure (CAS) with a space group O_h and a lattice constant of $a = 9.7691$ Å.[155] For ZnO, it possesses a hexagonal wurtzite-type structure (HWS) with the C_{6v} symmetry. The lattice constants are $a = 3.25$ Å and $c = 5.2$ Å; with a ratio of $c/a \sim 1.60$ close to the ideal value for hexagonal cell ($c/a = 1.633$). In both structures, the zinc ions are surrounded tetrahedrally by four anions. In the thermal annealing process, the oxygen atoms were adsorbed and diffuse into the Zn_3N_2 matrix via interstitial sites and were bonded to Zn, leading to structural phase changing from CAS to HWS. There were lots of defects, such as vacancies, interstitials, in the films during the transformation from CAS Zn_3N_2 to HWS ZnO. Usually, these kinds of defects could not be completely eliminated by annealing treatment. The ZnO p/n homojunction diode, in which p-ZnO is made by the RSD method, showed the wide EL spectrum, coving a range of 360–660 nm. This indicated that lots of defects exist in this ZnO p/n junction. The behavior of p-ZnO with light illumination also indicated that a high density of local states existed in ZnO prepared by oxidation of Zn_3N_2.[136] Additionally, as in most group II–VI materials, the bonding in ZnO is largely ionic (Zn^{2+}–O^{2-}) with the corresponding radii of 0.074 nm for Zn^{2+} and 0.140 nm for O^{2-}, respectively, leading to the generation of defects in the performance of ZnO-based devices. The main advantage of the RSD method is that the Zn–N bond is already formed in advance before synthesis of ZnO. However, the processes of O replacing N, accompanied by phase transformation in the thermal oxidizing, brought about substantial defects in ZnO. How to improve the structural quality of ZnO thin film but still with holding high N incroporation becomes a crucial issue in the RSD method, which needs figuring out. In ZnO and ZnSe materials, the hole densities have been increased by modulating the growth temperature or the delta doping methods.[22,156] For the ZnO material, the narrow window of epitaxial 2D growth also holds back the effective doping of acceptors. To avoid the growth degradation due to the introduction of acceptor dopants, a two zone growth method, i.e. alternate growth of intrinsic ZnO layer and N-doped layer, can be performed in the epitaxial growth. Note that the N-doped layer has a thickness of sub-monolayer, realized by controlling the surface reaction in the growth. If aluminum is also introduced into the surface reaction, several types of acceptors, like AlN2, AlN3, and AlN4 clusters, can be created on the ZnO surface with proper crystal orientation. The hole densities in ZnO are associated with the thickness of intrinsic ZnO layers and 2D areal densities of N or AlN_x ($x = 2$, 3, or 4) clusters. Furthermore, with the introduction of aluminum, the covalence of the chemical bond in the ZnO matrix is enhanced, which can suppress the formation of defects in the device running. In our experimental results, it has been found that the stabilities of electronic

and optical properties can be improved by introducing Al and N elements into ZnO.

3.3. Band gap engineering by controlling the O/N ratio in N–O based compounds

The band gap is an intrinsic characteristic of semiconductors and plays a central role in modern device physics & technology: it governs the operation of semiconductor devices. Generally, a tunable band gap is highly desirable because it would allow great flexibility in designing and optimizing the devices. One has successfully tuned the band gap and extended the range of their applications.[48–54,57,157] Initially, the RSD method was proposed to realize the p-type doping of ZnO. It has been demonstrated that it can sufficiently raise the solubility of the N acceptors in ZnO. However, looking at Fig. 3, the dominant efforts focused on the two extreme points of Zn_3N_2 and ZnO, as well as the annealing processes for the transformation from Zn_3N_2 to ZnO. The intermediate material of Zn–N–O ternary alloys has almost been ignored. Very recently, it has been identified that the Zn–N–O material system has promising potential applications,[158] in addition to amorphous InGaZnO,[159] in the thin film transistors. But so far, the optical properties of the Zn–N–O alloys have not attracted much attention yet.

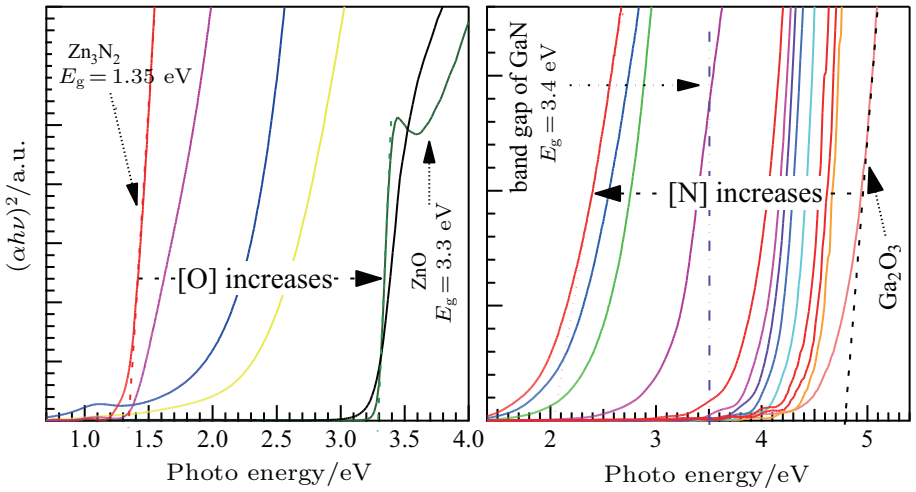


Fig. 10. (color online) Optical band gaps of N–O based compounds calculated from transmittance spectra with characteristic function, $(\alpha h\nu)^2 \propto h\nu - E_g$. Left: ZnNO ternary alloys with band gap tuning from 1.35 to 3.3 eV ($\Delta E = 1.95$ eV); right: GaON alloy with band gap tuning from 2.05 eV to 4.8 eV ($\Delta E = 2.75$ eV).

It has been known that the band gaps of Zn_3N_2 and ZnO are around 1.06 eV and 3.37 eV, respectively.[160] One possibility is that the band gap could be engineered in a range of 1.06–3.37 eV by tuning the ratio of N/O in the Zn–N–O ternary alloy. As shown in Fig. 10, on the left side are the recent experimental results on the band gap engineering of the Zn–N–O alloy prepared by megnetron sputtering technique. We can tune the band gap from 1.35 eV (band gap of Zn_3N_2) to 3.3 eV (ZnO). Note that the value of 1.35 eV is larger than 1.06 eV of the band gap of Zn_3N_2 single crystal thin film prepared by MBE. The slightly larger value in our sample is possibly attributed to the effect of residual oxygen in the chamber. Like TiO_2 material, ZnO is also known to be a good photocatalyst, which shows relatively high resistance to the degradation of several environmental contaminants under the irradiation of ultraviolet (UV) light ($\lambda < 374$ nm).[161–163] However, low efficiency for utilizing solar light hinders its final commercialization. With reducing the band gap of ZnO by incorporating N, more sunlight will be harvested and the efficiency of photocatalysis can be improved. The Ga_2O_3 is another versatile functional material with chemical and physical stabilities, which has been recognized as a promising candidate for solar blind UV photodetector, power devices, and photocatalysis in solar water splitting.[164–166] With a two-step nitridation method, we can introduce N into Ga_2O_3 to replace O. As a result, as shown on the right side of Fig. 10, we realize the band gap tuning from 4.8 eV to 2.05 eV. The huge spectral span of $\Delta E = 2.75$ eV is much larger than the expected value of 1.4 eV (4.8 $eV_{(Ga_2O_3)}$–3.4 $eV_{(GaN)}$). The reasons for band gap narrowing in N-alloyed Ga_2O_3 are related to N2p–Ga3d orbital repulsion and the formation of hexagonal phase. A detailed discussion can be found in our recent report.[76]

4. Conclusions and perspectives

With sustained efforts, the research on ZnO has achieved significant progress. Several novel ZnO-based emitters have been realized and enriched the concept of semiconductor lasers. However, the aspiration to realize high performance UV LEDs or UV lasers based on the ZnO p/n homojunction

has not been realised yet, because of the lack of high quality reproducible p-type ZnO. In this review paper, we introduce the RSD method, i.e., the thermal oxidizing Zn_3N_2 precursors, to synthetize p-type ZnO, which resolves the low solubility of N dopants and raises the N-acceptor concentration. The hole density up to 10^{19} cm^{-3} has been achieved in p-type ZnO prepared by the RSD method. The successes of this method have given constructive implications for the carrier doping processes and band gap engineering in the semiconductor industry.[147] Furthermore, the RSD method offers a path to overcoming the difficulty in anion-doping for not only ZnO, but also other wide bandgap oxide semiconductors like TiO_2, SnO_2, etc.

The thermal stability of p-type ZnO:(Al,N) has been improved with the introduction of Al into Zn_3N_2:Al precursor. In the thermal annealing process, the N could be stabilized and excessive replacement by O atoms can be avoided. The clusters of AlN_x ($x = 2, 3, 4$) as an acceptor in ZnO may be formed. Work on optimizing the relationship between the Al doping concentration in Zn_3N_2 precursor and carrier density of holes in p-ZnO is still in progress.

The band gap of an intermediate material, Zn–N–O ternary alloy, has been investigated by optical transmittances. We have tuned the band gap from 1.35 eV to 3.3 eV by controlling O atoms in the Zn–N–O material. We have also realized the huge range of band gap engineering from 2.05 eV to 4.8 eV in GaON with a two step nitridation method. The achievements of large band gap tunability with the introduction of N into oxide semiconductors indicate that the metal–N–O alloys have potential applications in photocatalysis for harvesting more visible light, and also enhance the flexibility of optoelectroic devices operating at selected wavelength in a wide range.

Acknowledgment

The authors sincerely thank Dr. Aidong Shen (Department of Electrical Engineering, The City College of New York, New York 10031, USA) for his invaluable advice on improving the manuscript.

References

[1] Ozgur U, Alivov Y I, Liu C, Teke A, Reshchikov M A, Dogan S, Avrutin V, Cho S J and Morkoc H 2005 *J. Appl. Phys.* **98** 041301
[2] Kozuka Y, Tsukazaki A and Kawasaki M 2014 *Appl. Phys. Rev.* **1** 011303
[3] Huang M H, Mao S, Feick H, Yan H Q, Wu Y Y, Kind H, Weber E, Russo R and Yang P D 2005 *Science* **292** 1897
[4] Bagnall D M, Chen Y F, Zhu Z, Yao T, Koyama S, Shen M Y and Goto T 1997 *Appl. Phys. Lett.* **70** 2230
[5] Zu, P, Tang Z K, Wang G K L, Kawasaki M, Ohotmo A, Koinuma H and Segawa H 1997 *Soli. State Com.* **103** 459
[6] Wiersma D S 2008 *Nat. Phys.* **4** 359
[7] Cao H, Zhao Y G, Ho S T, Seelig E W, Wang Q H and Chang R P H 1999 *Phys. Rev. Lett.* **82** 2278
[8] Que M L, Wang X D, Peng Y Y and Pan C F 2017 *Chin. Phys. B* **26** 067301
[9] Chu S, Wang G P, Zhou W H, Lin Y Q, Chernyak L, Zhao J Z, Kong J Y, Li L, Ren J J and Liu J L 2011 *Nat. Nano.* **6** 506
[10] Lu J F, Shi Z L, Wang Y Y, Lin Y, Zhu, Q X, Tian Z S, Dai J, Wang S F and Xu C X 2016 *Sci. Rep.* **6** 25645
[11] Ren X L, Zhang X H, Liu N S, Wen L, Ding L W, Ma Z W, Su J, Li LY, Han J B and Gao Y H 2015 *Adv. Fun. Mater.* **25** 2182
[12] Lu Y J, Li H F, Shan C X, Li B H, Shen D Z, Zhang L G and Yu S F 2014 *Opt. Exp.* **22** 17524
[13] Zhang X M, Lu M Y, Zhang Y, Chen L and Wang Z L 2009 *Adv. Mater.* **21** 2767
[14] Zhang Y T, Xia X C, Wu B, Shi Z F, Yang F, Yang X T, Zhang B L and Du G T 2014 *Chin. Phys. Lett.* **31** 058101
[15] Przezdziecka E, Stachowicz M, Chusnutdinow S, Jakieła R and Kozanecki A 2015 *Appl. Phys. Lett.* **106** 062106
[16] Klingshirn C, Fallert J, Zhou H, Sartor J, Thiele J, Thiele C, Maier-Flaig F, Schneider D and Kalt H 2010 *Phys. Sta. Soli. B* **247** 1424
[17] Özgür ü, Alivov Y I, Liu C, Teke A, Reshchikov M A, Doğan S, Avrutin V, Cho S J and Morkoç H 2005 *J. Appl. Phys.* **98** 041301
[18] Tang Z K, Wong G K L, Yu P, Kawasaki M, Ohtomo A, Koinuma H and Segawa Y 1998 *Appl. Phys. Lett.* **72** 3270
[19] Chen Y F, Bagnall D M, Koh H J, Park K T, Hiraga K, Zhu Z Q and Yao T 1998 *J. Appl. Phys.* **84** 3912
[20] Nakahara K, Akasaka S, Yuji H, Tamura K, Fujii T, Nishimoto Y, Takamizu D, Sasaki A, Tanabe T, Takasu H, Amaike H, Onuma T, Chichibu S F, Tsukazaki A, Ohtomo A and Kawasaki M 2010 *Appl. Phys. Lett.* **97** 013501
[21] Nie J C, Yang J Y, Piao Y, Li H, Sun Y, Xue Q M, Xiong C M, Dou R F and Tu Q Y 2008 *Appl. Phys. Lett.* **93** 173104
[22] Tsukazaki A, Ohtomo A, Onuma T, Ohtami M, Makino T, Sumiya M, Ohtani K, Chichibu S F, Fuke S, Segawa Y, Ohno H, Koinuma H and Kawasaki M 2005 *Nat. Mater.* **4** 42
[23] Jiao S J, Zhang Z Z, Lu Y M, Shen D Z, Yao B, Zhang J Y, Li B H, Zhao D X, Fan X W and Tang Z K 2006 *Appl. Phys. Lett.* **88** 031911
[24] Look D C, Claflin B, Alivov Y I and Park S J 2004 *Phys. Stat. Sol. (a)* **201** 2203
[25] Ryu Y, Lee T S, Lubguban J A, White H W, Kim B J, Park Y S and Youn C J 2006 *Appl. Phys. Lett.* **88** 241108
[26] Lu Y J, Shan C X, Zhou Z X, Wang Y L, Li B H, Qin J M, Ma H, Jia X P, Chen Z H and Shen D Z 2015 *Optica* **2** 558
[27] Nakamura T, Firdaus K and Adachi S 2012 *Phys. Rev. B* **86** 205103
[28] Nakamura T, Fujiwara H, Niyuki R, Sasaki K, Ishikawa Y, Koshizaki N, Tsuji T and Adachi S 2014 *New J. Phys.* **16** 093054
[29] Li Y P, Wang C X, Jin L, Ma X Y and Yang D R 2013 *J. Appl. Phys.* **113** 213103
[30] Fujiwara H, Niyuki R, Ishikawa Y, Koshizaki N, Tsuji T and Sasaki K 2013 *Appl. Phys. Lett.* **102** 061110
[31] Yu S F, Yuen C, Lau S P, Park W I and Yi G C 2004 *Appl. Phys. Lett.* **84** 3241
[32] Klingshirn C, Hauschild R, Fallert J and Kalt H 2007 *Phys. Rev. B* **75** 115203
[33] Lai Y Y, Chou Y H, Lan Y P, Lu T C, Wang S C and Yamamoto Y 2016 *Sci. Rep.* **6** 20581
[34] Bagnall D M, Chen Y F, Zhu Z, Yao T, Shen M Y and Goto T 1998 *Appl. Phys. Lett.* **73** 1038
[35] Gadallah A-S, Nomenyo K, Couteau C, Rogers D J and Lerondel G 2013 *Appl. Phys. Lett.* **102** 171105
[36] Lai Y Y, Chen J W, Chang T C, Chou Y H and Lu T C 2015 *Appl. Phys. Lett.* **106** 131106
[37] Wang Y F, Liao L M, Hu T, Luo S, Wu L, Wang J, Zhang Z, Xie W, Sun L X, Kavokin A V, Shen X C and Chen Z H 2017 *Phys. Rev. Lett.* **118** 063602
[38] Xie W, Dong H, Zhang S, Sun L, Zhou W, Ling Y, Lu J, Shen X C and Chen Z H 2012 *Phys. Rev. Lett.* **108** 166401
[39] Li F, Orosz L, Kamoun O, Bouchoule S, Brimont C, Disseix P, Guillet T, Lafosse X, Leroux M, Leymarie J, Mexis M, Mihailovic M, Patriarche G, Re'veret F, Solnyshkov D, Zuniga-Perez J and Malpuech G 2013 *Phys. Rev. Lett.* **110** 196406
[40] Czekalla C, Sturm C, Schmidt-Grund R, Cao B, Lorenz M and Grundmann M 2008 *Appl. Phys. Lett.* **92** 241102
[41] Wang Y Y, Xu C X, Jiang M M, Li J T, Dai J, Lu J F and Li P L 2016 *Nanoscale* **8** 16631

[42] Chen R, Ling B, Sun X W and Sun H D 2011 *Adv. Mater.* **23** 2199
[43] Zhang Y, Yan X Q, Yang Y, Huang Y H, Liao Q L and Qi J J 2012 *Adv. Mater.* **24** 4647
[44] Li P F, Liao Q L, Yang S Z, Bai X D, Huang Y H, Yan X Q, Zhang Z, Liu S, Lin P, Kang Z and Zhang Y 2014 *Nano Lett.* **14** 480
[45] Nakahara K, Akasaka S, Yuji H, Tamura K, Fujii T, Nishimoto Y, Takamizu D, Sasaki A, Tanabe T, Takasu H, Amaike H, Onuma T, Chichibu S F, Tsukazaki A, Ohtomo A and Kawasaki M 2010 *Appl. Phys. Lett.* **97** 013501
[46] Shen D Z, Mei Z X, Liang H L, Du X L, Ye J D, Gg S L, Wu Y X, Xu C X, Zhu G Y, Dai J, Chen M M, Ji X, Tang Z K, Shan C X, Zhang B L, Du G T and Zhang Z Z 2014 *Chin. J. Lum.* **35** 1
[47] Pearton S J, Norton D P, Ip K, Heo Y W and Steiner T 2005 *Progress in Materials Science* **50** 293
[48] Coughlan C, Schulz S, Caro M A and O'Reilly E P 2015 *Phys. Sta. Soli. B* **252** 879
[49] Vurgaftmana I, Meyer J R and Ram-Mohan L R 2001 *J. Appl. Phys.* **89** 5815
[50] Ryu Y R, Lee T S, Lubguban J A, Corman A B, White H W, Leem J H, Han M S, Park Y S, Youn C J and Kim W J 2006 *Appl. Phys. Lett.* **88** 052103
[51] Ju Z G, Shan C X, Jiang D Y, Zhang J Y, Yao B, Zhao D X, Shen D Z and Fan X W 2008 *Appl. Phys. Lett.* **93** 173505
[52] Hou Y N, Mei Z X, Liang H L, Gu C Z and Du X L 2014 *Appl. Phys. Lett.* **105** 133510
[53] Kalusniak S, Sadofev S, Puls J and Henneberger F 2009 *Laser & Photon Rev.* **3** 233
[54] Yang W F, Liu B, Chen R, Wong L M, Wang S J and Sun H D 2010 *Appl. Phys. Lett.* **97** 061911
[55] Zhao K L, Chen G P, Li B S and Shen A D 2014 *Appl. Phys. Lett.* **104** 212104
[56] Bellotti E, Driscoll K, Moustakas T D and Paiella R 2009 *J. Appl. Phys.* **105** 113103
[57] Su L X, Zhu Y, Yong D, Chen M, Ji X, Su Y, Gui X, Pan B, Xiang R and Tang Z 2014 *ACS Appl. Mater. Interfaces* **6** 14152
[58] Reynolds J G, Reynolds C L, Mohanta J A, Muth J F, Rowe J E, Everitt H O and Aspnes D E 2013 *Appl. Phys. Lett.* **102** 152114
[59] Pandey S K, Pandey S K, Awasthi V, Gupta M, Deshpande U P and Mukherjee S 2013 *Appl. Phys. Lett.* **103** 072109
[60] Lee J S, Cha S N, Kim J M, Nam H W, Lee S H, Ko W B, Wang K L, Park J G and Hong J P 2011 *Adv. Mater* **23** 4183
[61] Chen F G, Ye Z Z, Xu W Z, Zhao B H, Zhu L P and Lv J G 2005 *J. Crys. Growth* **281** 458
[62] Sui Y R, Yao B, Xiao L, Yang L L, Liu Y Q, Li F X, Gao M, Xing G Z, Li S and Yang J H 2012 *Thin Solid Films* **520** 5914
[63] Kim K K, Kim H S, Hwang D K, Lim J H and Park S J 2003 *Appl. Phys. Lett.* **83** 63
[64] Bian J M, Li X M, Gao X D, Yu W D and Chen L D 2004 *Appl. Phys. Lett.* **84** 541
[65] Heo Y W, Kwon Y W, Li Y, Pearton S J and Norton D P 2004 *Appl. Phys. Lett.* **84** 3474
[66] Tsukazaki A, Ohtomo A, Onuma T, Ohtani M, Makino T, Sumiya M, Ohtani K, Chichibu S F, Fuke S, Segawa Y, Ohno H, Koinuma H and Kawasaki M 2005 *Nat. Mater.* **4** 42
[67] Liu W, Gu S L, Ye J D, Zhu S M, Liu S M, Zhou X, Zhang R, Shi Y, Zheng Y D, Hang Y and Zhang C L 2006 *Appl. Phys. Lett.* **88** 092101
[68] Xu W Z, Ye Z Z, Zeng Y J, Zhu L P, Zhao B H, Jiang L, Lu J G, He H P and Zhang S B 2006 *Appl. Phys. Lett.* **88** 173506
[69] Ryu Y, Lee T S, Lubguban J A, White H W, Kim B J, Park Y S and Park Y S 2006 *Appl. Phys. Lett.* **88** 241108
[70] Wei Z P, Lu Y M, Shen D Z, Zhang Z Z, Yao B, Li B H, Zhang J Y, Zhao D X, Fan X W and Tang Z K 2007 *Appl. Phys. Lett.* **90** 042113
[71] Chu S, Olmedo M, Yang Z, Kong J and Liu J 2008 *Appl. Phys. Lett.* **93** 181106
[72] Choi Y S, Kang J W, Hwang D K and Park S J 2010 *IEEE Trans. Elect. Dev.* **57** 26
[73] Liu J S, Shan C X, Li B H, Zhang Z Z, Liu K W and Shen D Z 2013 *Opt. Lett.* **38** 2113
[74] Li B S, Liu Y C, Zhi Z Z, Shen D Z, Lu Y M, Zhang J Y, Fan X W, Mu R X and Henderson D O 2003 *J. Mater. Res.* **18** 8
[75] Wang Y F, Song D Y, Li L, Li B S, Shen A and Sui Y 2016 *Phys. Stat. Sol. C* **13** 585
[76] Song D Y, Li L, Li B. S, Sui Y and Shen A D 2016 *AIP Adv.* **6** 065016
[77] Wang L G and Zunger A 2003 *Phys. Rev. Lett.* **90** 256401
[78] Nian Q, Callahan M, Saei M, Look D, Efstathiadis H, Bailey J and Cheng G J 2015 *Sci. Rep.* **5** 15517
[79] Look D C, Leedy K D, Thomson D B and Wang B 2014 *J. Appl. Phys.* **115** 012002
[80] Sun H, Jen S U, Chen S C, Ye S S and Wang X 2017 *J. Phys. D: Appl. Phys.* **50** 045102
[81] Ellmer K 2012 *Nat. Photo.* **6** 809
[82] Janotti A and Van de Walle C G 2007 *Phys. Rev. B* **76** 165202
[83] Vanheusden K, Warren W L, Seager C H, Tallant D R, Voigt J A and Gnade B E 1996 *J. Appl. Phys.* **79** 7983
[84] Kim Y S and Park C H 2009 *Phys. Rev. Lett.* **102** 086403
[85] Li X N, Keyes B, Asher S, Zhang S B, Wei S H, Coutts T J, Limpijumnong S and Van de Walle C G 2005 *Appl. Phys. Lett.* **86** 122107
[86] McCluskey M D and Jokela S J 2009 *J. Appl. Phys.* **106** 071101
[87] Janotti A and Van de Walle C G 2007 *Phys. Rev. B* **76** 165202
[88] Robertson J and Clark S J 2011 *Phys. Rev. B* **83** 075205
[89] Makino T, Segawa Y, Tsukazaki A, Ohtomo A and Kawasaki M 2005 *Appl. Phys. Lett.* **87** 022101
[90] Vanheusden K, Seager C H, Warren W L, Tallant D R and Voigt J A 1995 *Appl. Phys. Lett.* **68** 15
[91] Korsunska N O, Borkovska L V, Bulakh B M, Khomenkova Y L, Kushnirenko V I and Markevich I V 2003 *J. Lum* **102** 733
[92] Leiter F, Alves H, Pfisterer D, Romanov N G, Hofmann D M and Meyer B K 2003 *Physica B* **340** 201
[93] Leiter F H, Alves H R, Hofstaetter A, Hofmann D M and Meyer B K 2001 *Phys. Stat. Sol. (b)* **226** R4
[94] Janotti A, Van de Walle C G 2006 *J. Crys. Growth* **287** 58
[95] Hofmann D M, Hofstaetter A, Leiter F, Zhou H, Henecker F, Meyer B K, Orlinskii S B, Schmidt J and Baranov P G 2002 *Phys. Rev. Lett.* **88** 045504
[96] Lyons J L, Steiauf D Janotti A and Van de Walle C G 2014 *Phys. Rev. Appl.* **2** 064005
[97] Park C H, Zhang S B and Wei S H 2002 *Phys. Rev. B* **66** 073202
[98] Kang H S, Ahn B D, Kim J H, Kim G H, Lim S H, Chang H W and Lee S Y 2006 *Appl. Phys. Lett.* **88** 202108
[99] Lee E C and Chang K J 2004 *Phys. Rev. B* **70** 115210
[100] Lim J H, Kang C K, Kim K K, Park I K, Hwang D K and Park S J 2006 *Adv. Mater.* **18** 2720
[101] Look D C, Reynolds D C, Litton C W, Jones R L, Eason D B and Cantwell G 2002 *Appl. Phys. Lett.* **81** 1830
[102] Yim K, Lee J, Lee D, Lee M, Cho E, Lee H S, Nahm H H and Han S 2017 *Sci. Rep.* **7** 40907
[103] Park R M, Troffer M, Rouleau C M, DePuydt J M and Haase M A 1990 *Appl. Phys Lett.* **57** 2127
[104] Liu W, Gu S L, Ye J D, Zhu S M, Liu S M, Zhou X, Zhang R, Shi Y, Zheng Y D, Hang Y and Zhang C L 2006 *Appl. Phys. Lett.* **88** 092101
[105] Barnes T M, Olson K and Wolden C A 2005 *Appl. Phys. Lett.* **86** 112112
[106] Rakhshani A E 2017 *J. Alloy. Compound.* **695** 124
[107] Tsukazaki A, KUBOTA M, Ohtomo A, Onuma T, Ohtani K, Ohno H, Chichibu S F and Kawasaki M 2004 *Jpn J. Appl. Phys.* **44** L643
[108] Liu J S, Shan C X, Shen H, Li B H, Zhang Z Z, Liu L, Zhang L G and Shen D Z 2012 *Appl. Phys. Lett.* **101** 011106
[109] Li D H, Wang H Q, Zhou H, Li Y P, Huang Z, Zheng J C, Wang J O, Qian H J, Ibrahim K, Chen X H, Zhan H H, Zhou Y H and Kang J Y 2016 *Chin. Phys. B* **25** 076105
[110] Lyons J L, Janotti A and Van de Walle C G 2009 *Appl. Phys. Lett.* **95** 252105
[111] Tarun M C, Zafar I M and McCluskey M D 2011 *AIP Adv.* **1** 022105
[112] Liu L, Xu J L, Wang D D, Jiang M M, Wang S P, Li B H and Zhang Z Z 2012 *Phys. Rev. Lett.* **108** 215501
[113] Reynolds J G, Reynolds C L, Mohanta A, Muth J F, Rowe J E, Everitt H O and Aspnes D E 2013 *Appl. Phys. Lett.* **102** 152114
[114] Limpijumnong S, Zhang S B, Wei S H and Park C H 2004 *Phys. Rev. Lett.* **92** 155504
[115] Chadi D J 1991 *Appl. Phys. Lett.* **59** 3589
[116] Chen F G, Ye Z Z, Xu W Z, Zhao B H, Zhu L P and Lv J G 2005 *J. Crys. Growth* **281** 458
[117] Jeong T S, Yu J H, Mo H S, Kim T S, Youn C J and Hong K J 2013 *J. Appl. Phys.* **114** 053504

[118] Pandey S K, Pandey S K, Awasthi V, Gupta M, Deshpande U P and Mukherjee S 2013 *Appl. Phys. Lett.* **103** 072109

[119] Yim K, Lee J, Lee D, Lee M, Cho E, Lee H S, Nahm H H and Han S 2017 *Sci. Rep.* **7** 40907

[120] Ryu Y, Lee T S, Lubguban J A, White H W, Kim B J, Park Y S and Youn C J 2006 *Appl. Phys. Lett.* **88** 241108

[121] Ryu Y R, Lubguban J A and Lee T S, White H W, Jeong T S, Youn C J and Kim B J 2007 *Appl. Phys. Lett.* **90** 131115

[122] Liang J K, Su H L, Chuang P Y, Kuo C L, Huang S Y, Chan T S, Wu Y C and Huang J C A 2015 *Appl. Phys. Lett.* **106** 212101

[123] Janotti A and Van de Walle C G 2009 *Rep. Prog. Phys.* **72** 126501

[124] Yan Y F, Al-Jassim M M and Wei S H 2006 *Appl. Phys. Lett.* **89** 181912

[125] Ortega J J, Ortiz-Hernández A A, Berumen-Torres J, Escobar-Galindo R, Méndez-García V H and Araiza J J 2016 *Mater. Lett.* **181** 12

[126] Aimouch D E, Meskine S, Benaissa C Y, Zaoui A and Boukortt A 2017 *Optik* **130** 1320

[127] Ye Z, Wang T, Wu S, Ji X H and Zhang Q Y 2017 *J. All. Comp.* **690** 189

[128] Jaisutti R, Lee M, Kim J, Choi S, Ha T J, Kim J, Kim H, Park S K and Kim Y H 2017 *ACS Appl. Mater. Interfaces* **9** 8796

[129] Aimouch D E, Meskine S, Hayn R, Zaoui A and Boukortt A 2016 *Mod. Phys. Lett. B* **30** 1650291

[130] Bousmaha M, Bezzerrouk M A, Baghdad R, Chebbah K, Kharroubi B and Bouhafs B 2016 *Acta Phys. Polon. A* **129** 1155

[131] Garces N Y, Wang L, Bai L, Giles N C, Halliburton L E and Cantwell G 2002 *Appl. Phys. Lett.* **81** 622

[132] Patino R, Campos M and Torres L A 2007 *Inorg. Chem.* **46** 9332

[133] "Lange's Handbook of Chemistry" Sixteenth Edition, Section 4: PROPERTIES OF ATOMS, RADICALS, AND BONDS, Edited by Speight J G 4.5 bond lengths and strengths, p 4.41

[134] Ma J G, Liu Y C, Mu R, Zhang J Y, Lu Y M, Shen D Z and Fan X W 2004 *J. Vac. Sci. Technol. B* **22** 94

[135] Wang D, Liu Y C, Mu R, Zhang J Y, Lu Y M, Shen D Z and Fan X W 2004 *J. Phys.: Condens. Matter* **16** 4635

[136] Xiao Z Y, Liu Y C, Mu R, Zhao D X and Zhang J Y 2008 *Appl. Phys. Lett.* **92** 052106

[137] Xiao Z Y, Liu Y C, Zhang J Y, Zhao D X, Lu Y M, Shen D Z and Fan X W 2005 *Semicon. Sci. Technol.* **20** 796

[138] Barnes T M, Olson K and Wolden C A 2005 *Appl. Phys. Lett.* **86** 112112

[139] Butkuzi T V, Chelizde T G, Georgobiani A N, Jashiashvili D L, Khulordava T G and Tsekvava B E 1998 *Phys. Rev. B* **58** 10692

[140] Liu Z W, Yeo S W and Ong C K 2007 *J. Mater. Res.* **22** 2668

[141] Allenic A, Guo W, Chen Y B, Zhao G Y, Pan X Q, Che Y, Hu Z D and Liu B 2007 *J. Mater. Res.* **22** 2339

[142] Nakano Y, Morikawa T, Ohwaki T and Taga Y 2006 *Appl. Phys. Lett.* **88** 172103

[143] Jiang N K, Georgiev D G, Wen T and Jayatissa A H 2012 *Thin Solid Films* **520** 1698

[144] Zou C W, Chen R Q and Gao W 2009 *Sol. Sta. Comm.* **149** 2085

[145] Pakhshani A E, Bumajdad A, Kokaj J and Thomas S 2014 *Kuwait J. Sci.* **41** 107

[146] Erdogan N H, Kara K, Ozdamar H, Esen R and Kavak H 2013 *Appl. Sur. Sci.* **271** 70

[147] Jiang N K, Georgiev D G and Jayatissa A H 2013 *Semicond. Sci. Technol.* **28** 025009

[148] Kaminska E, Piotrowska A, Kossut J, Barcz A, Butkute R, Dobrowolski W, Dynowska E, Jakiela R, Przezdziecka E, Lukasiewicz R, Aleszkiewicz M, Wojnar P and Kowalczyk E 2005 *Soli. Sta. Comm.* **135** 11

[149] Wang C, Ji Z G, Liu K, Xiang Y and Ye Z Z 2003 *J. Crys. Grow.* **259** 279

[150] Jin Y P, Zhang B, Wang J Z and Shi L Q 2016 *Chin. Phys. Lett.* **33** 058101

[151] Wang L G and Zunger A 2003 *Phys. Rev. Lett.* **90** 256401

[152] Huda M N, Yan Y F and Al-Jassin M M 2012 *J. Phys.:Cond. Mat.* **24** 415503

[153] Tang X, Deng Y Z, Wagner D, Yu L and Lü H F 2012 *Sol. Stat. Com.* **152** 1

[154] Yamamoto T 2002 *Thin Solid Films* **420** 100

[155] Partin D E, Williams D J and O'Keeffe M 1997 *J. Sol. Sta. Chem.* **132** 56

[156] Zhang Q, Shen A D, Kuskovsky I L and Tamargo M C 2011 *J. Appl. Phys.* **110** 034302

[157] Kasai J I, Akimoto R, Hasama T, Ishikawa H, Fujisaki S, Tanaka S and Tsuji S 2011 *Appl. Phys. Exp.* **4** 082102

[158] Kim H S, Jeon S H, Park J S, Kim T S, Son K S, Seon J B, Seo S J, Kim S J, Lee E, Chung J G, Lee H, Han S, Ryu M, Lee S Y and Kim K 2013 *Sci. Rep.* **3** 1459

[159] Nomura K, Ohta H, Takagi A, Kamiya T, Hirano M and Hosono H 2004 *Nature* **432** 488

[160] Suda T and Kakishita K 2006 *J. Appl. Phys.* **99** 076101

[161] Hernandez-Alonso M D, Fresno F, Suarez S and Coronado J M 2009 *Energy Environ. Sci.* **2** 1231

[162] Yang L Y, Dong S Y, Sun J H, Feng J L, Wu Q H and Sun S P 2010 *J. Hazard. Mater.* **179** 438

[163] Kwiatkowski M, Chassagnon R, Heintz O, Geoffroy N, Skompska M and Bezverkhyy I 2017 *Appl. Cataly. B: Environmental* **204** 200

[164] Suzuki R, Nakagomi S and Kokubuna Y 2011 *Appl. Phys. Lett.* **98** 131114

[165] Higashiwaki M, Sasaki K, Kamimura T, Wong M H, Krishnamurthy D, Kuramata A, Masui T and Yamakoshi S 2013 *Appl. Phys. Lett.* **103** 123511

[166] Wang X, Shen S, Jin S Q, Yang J X, Li M R, Wang X L, Han H X and Li C 2013 *Phys. Chem. Chem. Phys.* **15** 19380